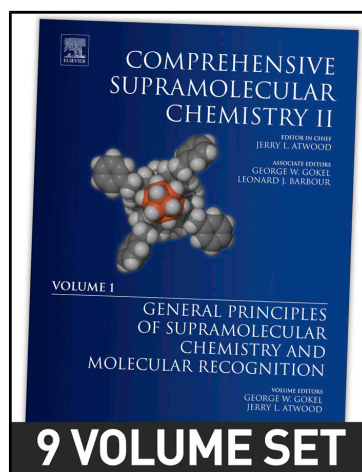


**Provided for non-commercial research and educational use.
Not for reproduction, distribution or commercial use.**

This article was originally published in Comprehensive Supramolecular Chemistry II, published by Elsevier, and the attached copy is provided by Elsevier for the author's benefit and for the benefit of the author's institution, for non-commercial research and educational use including without limitation use in instruction at your institution, sending it to specific colleagues who you know, and providing a copy to your institution's administrator.



All other uses, reproduction and distribution, including without limitation commercial reprints, selling or licensing copies or access, or posting on open internet sites, your personal or institution's website or repository, are prohibited. For exceptions, permission may be sought for such use through Elsevier's permissions site at:

<https://www.elsevier.com/about/our-business/policies/copyright/permissions>

From Lisbjerg, M.; Pittelkow, M. (2017) Hemicucurbit[*n*]urils. In: Atwood, J. L., (ed.) Comprehensive Supramolecular Chemistry II, vol. 3, pp. 221–236. Oxford: Elsevier.

ISBN: 9780128031988

Copyright © 2017 Elsevier Ltd. All rights reserved.
Elsevier

3.09 Hemicucurbit[*n*]urils

M Lisbjerg and M Pittelkow, University of Copenhagen, Copenhagen, Denmark

© 2017 Elsevier Ltd. All rights reserved.

3.09.1	Introduction	221
3.09.2	<i>En route</i> to Hemicucurbit[<i>n</i>]urils	222
3.09.3	Hemicucurbit[<i>n</i>]uril	222
3.09.4	Cyclohexylhemicucurbit[6]uril	225
3.09.5	Bambus[6]uril	227
3.09.6	Biotin[6]uril	230
3.09.7	Outlook	235
References		236

3.09.1 Introduction

Hemicucurbit[*n*]urils (eg, hemicucurbit[6]uril, **Fig. 1A**) are macrocyclic structures synthesized from an acid-catalyzed condensation reaction of an *N,N'*-dialkylurea and formaldehyde (or other aldehydes, but only formaldehyde has been used to date).¹ The name “hemicucurbituril” is derived from the name of another type of macrocycle, the cucurbit[*n*]uril, which is a structure synthesized from an acid-catalyzed condensation reaction of a glycoluril with formaldehyde (**Fig. 1B**).² The “cucurbit[6]uril” was named by Mock and coworkers due to the apparent structural resemblance between the 3D structure of the cucurbit[6]urils and the physical appearance of a pumpkin family (Cucurbitaceae).³ In 2004, when Miyahara and coworkers described the first hemicucurbit[*n*]urils,

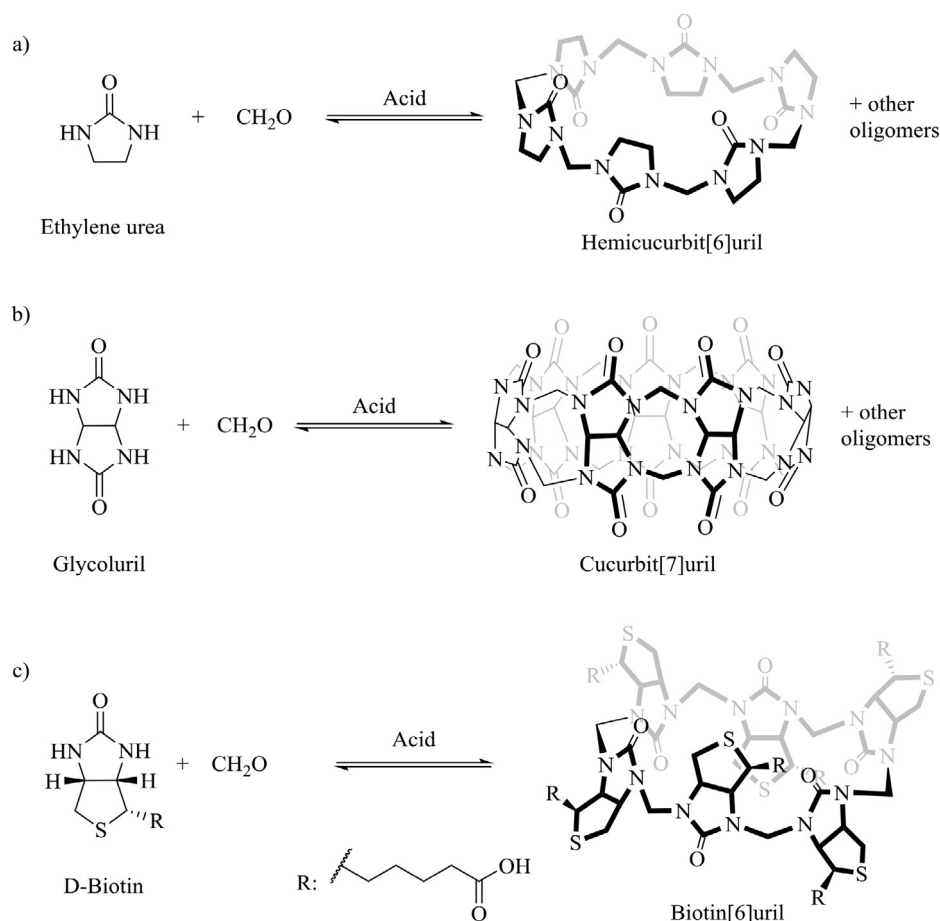


Figure 1 (A) Synthesis of hemicucurbit[6]uril by condensation of ethylene urea and formaldehyde. (B) Synthesis of cucurbit[7]uril by condensation of glycoluril and formaldehyde. (C) Synthesis of biotin[6]uril by condensation of D-biotin and formaldehyde.

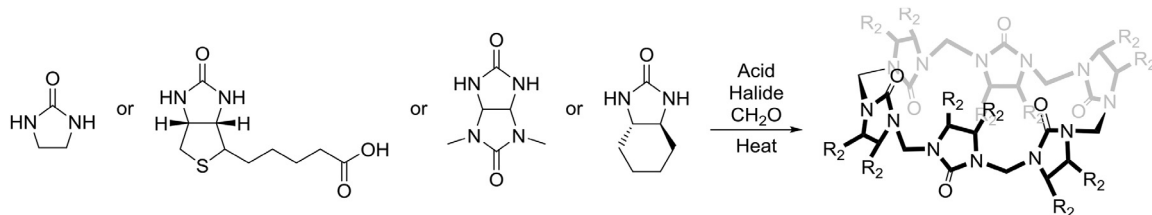


Figure 2 The different building blocks ethylene urea, D-biotin, 2,4-dimethyl-glycouril, and (*S,S*)-cyclohexyl urea, all give the same general motif of the hemicucurbit[6]uril, when using similar conditions.

they were named that way simply because the structure of one of the building blocks, ethylene urea, could be viewed, roughly, as a half glycouril building block that is used to prepare cucurbit[*n*]urils.

In Miyahara's pioneering work, a number of hemicucurbit[*n*]urils were prepared and a number of interesting observations and trends observed. Almost all of the hexameric macrocycles in the hemicucurbit[*n*]uril family bind anions in the cavity through C—H···anion interactions.^{1,4–6} This is in contrast to the cucurbit[*n*]urils that tend to bind cations largely through dipole cation interactions.^{7–9} All the members of the hemicucurbit[6]uril family described so far have been synthesized through a templated condensation reaction between the desired *N,N'*-dialkyl urea monomer, formaldehyde, and the corresponding halide anion that works as a template, yielding the macrocyclic structure (Fig. 2). New analogs include Sindelar and coworker's bambus[6]uril,⁴ our own biotin [6]uril,⁵ and the cyclohexylhemicucurbit[6]uril described by Aav and coworkers.⁶

Especially the anion-binding properties of the hemicucurbit[6]urils have achieved significant attention.^{10,11} The hexameric structures exhibit strong binding to anions, for example, iodide, both in water and in organic solvents depending on the specific hemicucurbit[6]uril.^{4,12–14} These strong binding affinities have been obtained purely by C—H···anion interactions, and it has been speculated that a chaotropic effect and/or the nonclassical hydrophobic effect is involved in achieving high binding affinities.^{13,15} The intriguing structures of the macrocycles have inspired their use as anionophores,¹⁴ catalysts,¹⁶ and oxidation vessels.^{17,18}

3.09.2 En route to Hemicucurbit[*n*]urils

The first hemicucurbit[*n*]uril was described in 2004 by Miyahara and coworkers (Fig. 1). The original synthetic work was inspired by the vast bulk of work describing the synthesis and properties of cucurbit[*n*]urils. When considering ethylene urea as “half” a glycouril, the transfer of logic from the cucurbit[*n*]urils to the hemicucurbit[*n*]urils seems apparent, and initially the original expectations were also that the supramolecular binding properties of the hemicucurbit[*n*]urils would be similar to those of the cucurbit[*n*]urils.

Glycouril was used as early as 1905 by Behrend et al. to prepare a polymer by reaction with formaldehyde, and it was much later (1981) discovered that it was possible to prepare the corresponding macrocycles, the cucurbit[6]urils (eg, CB[6]), by a similar synthetic procedure.

To fully appreciate the unique supramolecular chemistry of the cucurbit[*n*]urils, it is illustrative to consider the structural features of the CB[6] (Fig. 3). CB[6] is a macrocycle composed of 6 glycourils connected by 12 methylene bridges. This gives CB[6] a hydrophobic cavity, and two polar entry portals. This construction is ideal for binding of, for example, the ammonium ions of α,ω -alkanediamines, where the cations are located at the portals of the CBs, and the alkyl chain is situated inside the hydrophobic cavity. When viewing each glycouril unit, they each have a convex side and a concave side, where the convex side has the two methine protons. In CB[6], each glycouril has the convex side pointing outward from the cavity and the methine protons therefore point away from the hydrophobic cavity.

The use of urea-containing molecules in supramolecular chemistry has been explored extensively in the past decades.^{19,20} The cucurbit[*n*]uril family of macrocycles has gained significant popularity in recent years due to the possibility of preparing strong binary and ternary complexes in water.⁸ The possibility to prepare ternary complexes with large binding affinities in water has been used in a number of chemical biology applications.^{21,22} The chemistry of glycouril-containing structures has also been scrutinized by Nolte and coworkers in their elegant studies, which has led to many applications in biological and materials chemistry.¹⁹

In this book chapter, we discuss the recent progress of macrocycles prepared from condensation of *N,N'*-dialkyl ureas, and their thio analogs, with formaldehyde. The review is organized in a fashion such that each macrocycle is described first including the synthesis followed by an analysis of their structures. Then an evaluation of the properties of the various macrocycles, for example, anion binding or catalysis, is presented.

3.09.3 Hemicucurbit[*n*]uril

The original, and so far structurally most simple of these hemicucurbit[*n*]uril macrocycles is the hemicucurbit[6]uril (hmCB[6]), which Miyahara and coworkers obtained by reacting ethylene urea and formalin in aqueous 4 M HCl at room temperature for 30 min (Fig. 4).¹

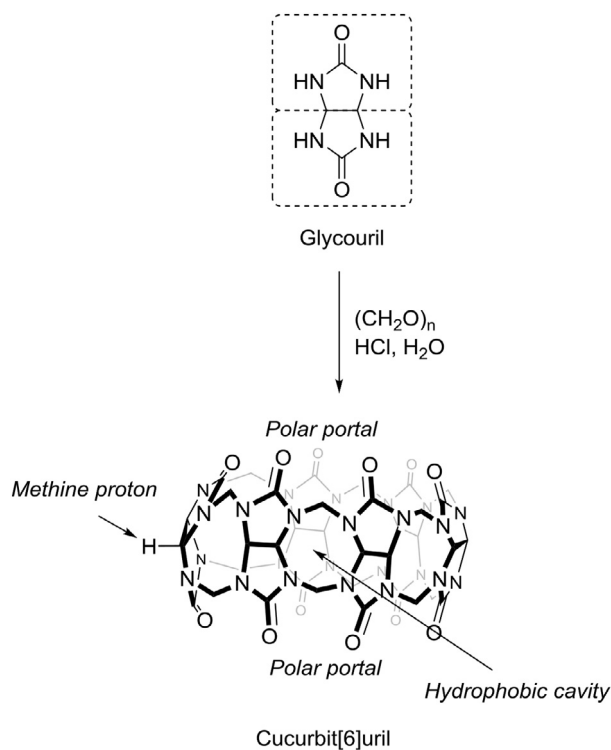


Figure 3 *Top:* Glycouril, the stippled line indicating the two “fused” ethylene ureas. *Bottom:* The main CB[6] macrocyclic products formed when reacting glycouril in aqueous HCl. Key structural features are highlighted.

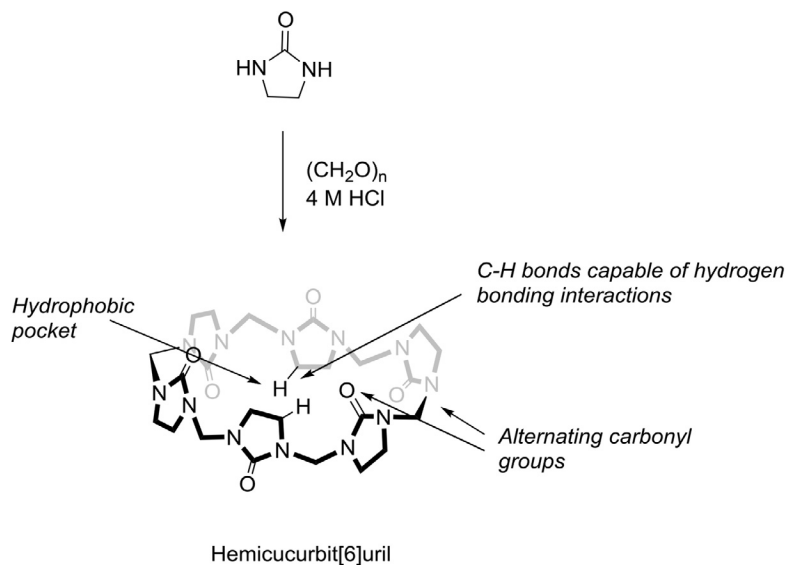


Figure 4 Synthesis of hemicucurbit[6]uril. Key structural features are highlighted.

From the reaction mixture, hmCB[6] precipitated as an HCl adduct, which was isolated in 94% yield. The hmCB[6] was the first of the macrocycles with the alternating configuration of the urea moieties, which was seen from the single crystal X-ray structure (Fig. 5). This alternating configuration is opposite of what has been observed in the CB[*n*]s, where the aligned carbonyls play an important role in the host–guest chemistry. This alternating orientation makes metal–ion bonding nonfeasible, but the structure does form a hydrophobic cavity that has been shown to interact favorably with anions through C–H⋯anion interactions.

The hmCB[6] can be viewed as a CB[6] cut in half at the equator, where the carbonyls of the ethylene urea units are arranged in alternating fashion. This alternating structure is probably the reason that hmCB[6] has no significant interaction with the cations

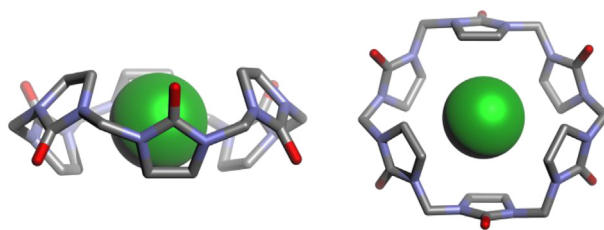


Figure 5 Hemicucurbit[6]uril single crystal X-ray structure with alternating orientation of the ethylene urea subunits (*left*: side view, *right*: top view). A chloride is situated in the cavity of the macrocycle, bound by C–H anion interactions.¹ Hydrogens atoms and solvent molecules have been removed for clarity.

like Na^+ , K^+ , NH_4^+ , Rb^+ , or Cs^+ , but instead interacts with SCN^- and I^- and some transition metal ions like Co^{2+} , UO^{2+} , and Ni^{2+} .^{10,11} This is very different from the CB[6] that binds cations, but not anions.^{7,8}

HmCB[6] has a low solubility in water, but taking advantage of the binding of, for example, thiocyanate, the solubility can be increased from 0.03 to 250 mg L^{-1} in water, by the addition of excess thiocyanate.^{1,10}

Furthermore, Miyahara and coworkers showed that it was possible to synthesize the hemicucurbit[12]uril (hmCB[12]) by changing the concentration of HCl from 4 to 1 M, using either the same starting materials as for the hmCB[6] or a polymer of ethylene urea and formaldehyde. The fact that the hmCB[12] can be formed either from the polymer or from the two components of the polymer shows that the reaction between ethylene urea and formaldehyde is reversible under the acidic reaction conditions used.

The hmCB[12] has a similar alternating orientation of the ethylene urea carbonyls as seen in the crystal structure of hmCB[6] (Figs. 5 and 6). The cavity of the hmCB[12] is larger than the cavity of hmCB[6] and the orientation of the ethylene urea carbonyls is not as strictly alternating as in the hmCB[6]. HmCB[12] has not been reported to bind anions.

In 2012, hmCB[6] was shown to catalyze the esterification of several conjugated carboxylic acids, but not simple alkyl carboxylic acids (Fig. 7).¹⁶ The authors found that hmCB[6] caused more effective catalysis of the smaller conjugated systems than larger ones, and they speculate that the mechanism of the reaction is a solvolysis.

Furthermore, they showed that the hmCB[12] did not have any catalytic effect, perhaps due to the larger size of the cavity. In a later paper by Yamato and coworkers, it was shown that hmCB[6] was able to catalyze the oxidation of furan, 2-methylfuran, and thiophene in water, using only the naturally occurring oxygen in the reaction mixture (Fig. 8).¹⁷

They also tested the hmCB[12], CB[6], and CB[7], but no catalysis of the oxidation reaction was observed. It was found that the hmCB[6] oxidation is faster when the pH is lowered from 6.3 to 2.0, and the authors speculate that the reaction mechanism starts with a protonation of the hmCB[6], which enables the macrocycle to bind furan within the cavity, and thereby enable the oxidation with O_2 . It appears unlikely that a complex would form within the cavity of the neutral macrocycle, as this has only been reported to bind anions. In 2013, hmCB[6] was shown to direct the oxidation of different hydroxybenzyl alcohols in the presence of 2-iodoxybenzoic acid (IBX) to the corresponding aldehyde without over oxidation (Fig. 9).¹⁸

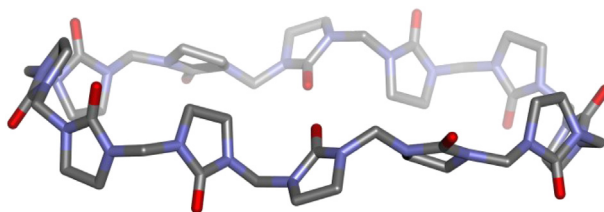


Figure 6 Side view of the single crystal X-ray structure of hmCB[12] showing the alternating orientation of the ethylene ureas.¹ Solvent molecules and hydrogen have been removed for clarity.

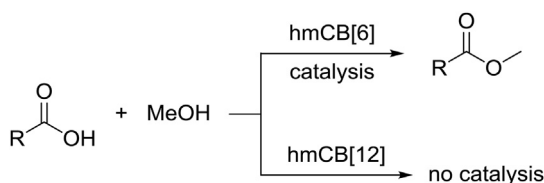


Figure 7 Esterification of conjugated carboxylic acids, catalyzed by hemicucurbit[6]uril under neutral conditions. The hmCB[12] does not catalyze the esterification, due to its larger size.

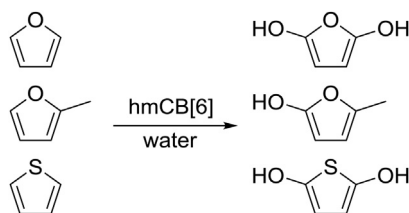


Figure 8 Oxidation by hmCB[6] in water.

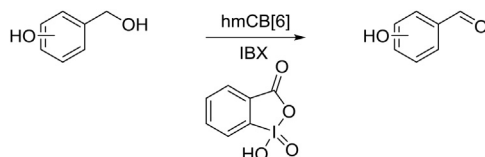


Figure 9 Oxidation by IBX in the presence of hmCB[6] which enables selective oxidation to the aldehyde of benzylic alcohols.

It was further shown that both steric and inductive effects affect the rate of oxidation, as 2-hydroxybenzyl alcohol reacts slowly and gives lower yields than that of 3- and 4-hydroxybenzyl alcohol.

By expanding the hmCB[6] ability to bind ions, Yamato and coworkers showed that hmCB[6] is able to bind the phenazine-HCl salt in a 1:1 ratio in a mixture of $\text{CHCl}_3/\text{MeOH}$.²³ Further, they showed that the hmCB[12] produces a 2:1 complex with phenazine-HCl salt due to its larger cavity and more flexible structure than hmCB[6].

3.09.4 Cyclohexylhemicucurbit[6]uril

In 2009, Wu and coworkers mixed the urea of (*R,S*)-cyclohexane urea and 1 equivalent of paraformaldehyde in 4 M HCl followed by heating at 70 °C for 4 h (Fig. 10).²⁴ The *meso*-cyclohexylhemicucurbit[6]uril (*meso*-cychmCB[6]) was isolated by column chromatography in 78% yield.

From the single crystal X-ray structure it was found that the *meso*-cychmCB[6] had the alternating orientation of carbonyl groups (Fig. 11) just as hmCB[6] has, and that it could include CHCl_3 or CCl_4 in the cavity. If on the other hand the crystals were grown from CH_2Cl_2 , instead of CHCl_3 or CCl_4 , the CH_2Cl_2 was located outside the cavity. Hydrogen bonding from methylene chloride to the urea carbonyl groups dominated the crystal packing of this structure.

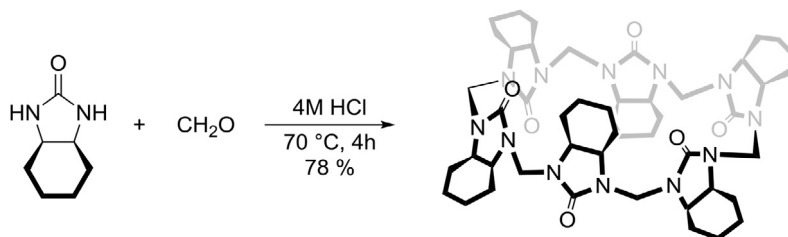


Figure 10 Synthesis of *meso*-cyclohexylhemicucurbit[6]uril.

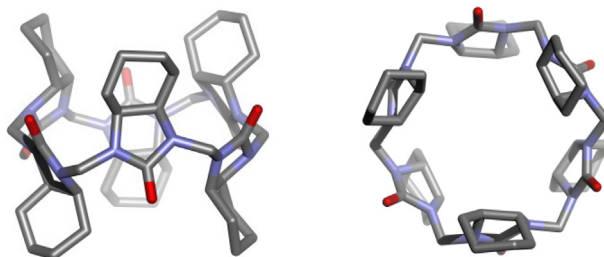


Figure 11 Single crystal X-ray structure of the *meso*-cyclohexylhemicucurbit[6]uril with alternating orientation of the dialkyl *N,N*-ethylene ureas (left: side view, right: top view).²⁴ Hydrogens and solvent molecules have been omitted for clarity.

The first enantiomerically pure members of the hemicucurbit[*n*]uril family were described in 2013, when Aav and coworkers produced the (*all-S*)-cyclohexylhemicucurbit[6]uril (*all-S*-cychmCB[6]) and (*all-R*)-cyclohexylhemicucurbit[6]uril (*all-R*-cychmCB[6]) using the previously reported synthetic procedure, employing either 4 M HCl or 4 M HBr, from which yields of 85% and 64% were obtained, respectively.⁶ The products were isolated by filtration of the precipitate, and the product was the HCl or the HBr complex depending on the acid used in the synthesis.

Again these structures had the alternating orientation of the cyclohexylurea monomeric units, and the macrocycles were shown to bind halide anions and carboxylates in CHCl₃ (Fig. 12). Unlike the *meso*-cychmCB[6] and the hmCB[6], which each have 12 methine groups where the hydrogen is pointing toward the cavity, (*all-S*)- and (*all-R*)-cychmCB[6] only has 6 of these hydrogens pointing toward the cavity due to the identical configuration of the two methine groups in the monomeric unit.

The (*all-S*)- or (*all-R*)-cychmCB[6] bound planar conjugated carboxylic acids tighter than carboxylic acids that were branched at the α position, probably due to steric congestion in the inclusion complex. Calculations, in gas phase, on the (*all-S*)-cychmCB[6]uril showed that the anions preferred to be located inside the cavity of cyclohexylhemicucurbit[6]uril and that the binding affinity of the anions in gas phase is $\text{Cl}^- > \text{Br}^- > \text{HCOO}^- > \text{I}^-$.²⁵ This trend was also confirmed by ion-mobility mass spectrometry. In 2014, the existence of even larger macrocycles of cyclohexylhemicucurbit[*n*]uril (*n* = 7–10) were shown to exist by analyzing the reaction mixture of (*all-R*)-cychmCB[6] by HPLC-MS.²⁶ The authors were able to isolate the (*all-R*)-cyclohexylhemicucurbit[8]uril (*all-R*-cychmCB[8]) in 11% yield by preparative HPLC. The *all-R*-cychmCB[8] was detected in negative-mode MS with either a chloride or a formate anion, showing its ability to bind anions in the gas phase.

In 2015, Aav and coworkers further optimized the synthesis of the (*all-R*)-cychmCB[8] by employing different anions such as HCO_2^- , CF_3CO_2^- , PF_6^- as the templates, and thereby increased the yield from 11% to 55–90% depending on the anion, and conditions used (Fig. 13).²⁷ The authors were able to synthesize the (*all-R*)-cychmCB[8] starting from either the (*R,R*)-cyclohexane urea and paraformaldehyde or from the (*all-R*)-cychmCB[6], which again shows the reversibility of the amination exchange reaction in acidic conditions.

From the crystal structure in Fig. 14, it is again evident that the macrocycle had an alternating orientation of the monomeric units, and that the cavity of the (*all-R*)-cychmCB[8] has a hydrophobic cavity. By diffusion (DOSY) NMR they showed that the macrocycle was able to bind anions, such as HCO_2^- , CF_3CO_2^- , and CH_3CO_2^- in CDCl₃ with similar affinities as the (*all-R*)-cyclohexylhemicucurbit[6]uril.

Sindelar and Fiala synthesized the norbornahemi[6]cucurbiturils, which can be viewed as a cyclohexylhemicucurbit[6]uril with a methylene bridge added to the cyclohexyl ring (Fig. 15).²⁸ By MS they also detected the norbornahemicucurbit[4, 5, 7, and 8]urils.

The norbornahemicucurbit[6]uril macrocycle was prepared from 4 M HCl at 70°C in 9% yield. They furthermore tried to change the reaction solvent to chloroform, but even with the addition of a template like iodide, they did not observe the desired macrocyclic product. Unlike many of the hexameric macrocycles with alternating orientation of the ethylene urea groups, no anion binding has been reported for the norbornahemicucurbit[6]uril.

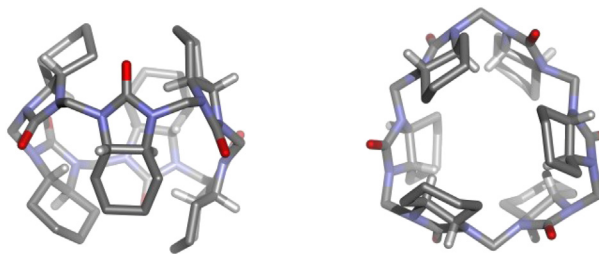


Figure 12 Single crystal X-ray structure of the (*all-S*)-cyclohexylhemicucurbit[6]uril (left: side view, right: top view).⁶ Solvent molecules have been omitted, and only methine hydrogens are shown for clarity.

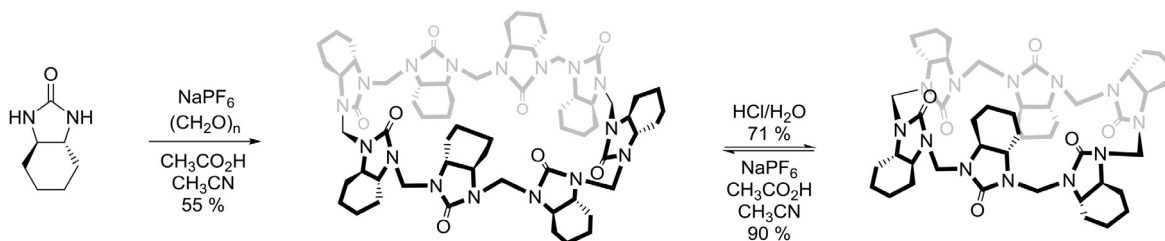


Figure 13 Synthetic pathways for the (*all-R*)-cyclohexylhemicucurbit[8]uril starting from the (*R,R*)-cyclohexane urea or (*all-R*)-cyclohexylhemicucurbit[6]uril.

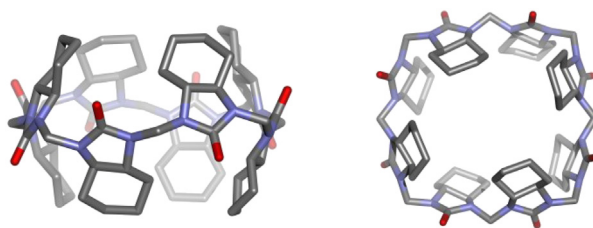


Figure 14 Single crystal X-ray structure of the (*all-S*)-cyclohexylhemicucurbit[8]uril (*left*: side view, *right*: top view).²⁷ Solvent molecules and hydrogens have been omitted for clarity.

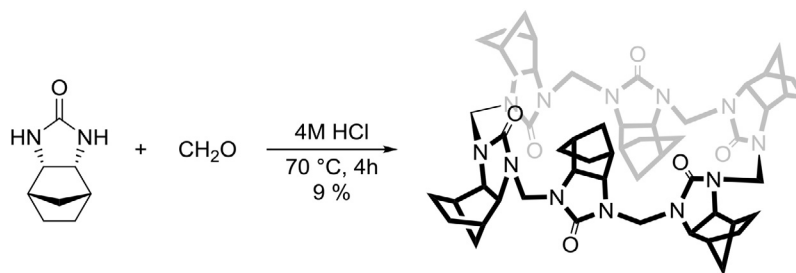


Figure 15 Norbornahemicucurbit[6]uril synthesis.

3.09.5 Bambus[6]uril

A new family of macrocycles was described in 2010 by Sindelar and coworkers, when they presented their bambus[6]uril (bam[6]), consisting of six glycouril monomers, which was capped with methyl groups at both nitrogen atoms on one of the urea groups, and connected through methylene bridges at the other urea (Fig. 16).⁴

They reacted 2,4-dimethyl-glycouril with formaldehyde in 5.4 M HCl, which produced the hexameric macrocycle containing one HCl molecule in 30% yield. The removal of HCl turned out to be tricky, but replacing the Cl^- with I^- , followed by oxidation of the I^- to I_3^- caused the bam[6] to precipitate without guest.²⁹ Removing the iodide from the bam[6] forces the macrocycle to precipitate anion-free, as the solubility of anion-free bam[6] is very low in common organic solvents. From single crystal X-ray analysis, it was shown that the bam[6] had the alternating orientation of the dialkyl-*N,N'*-ethylene urea groups, and it was shown that the macrocycle could bind BF_4^- , I^- , Br^- , and Cl^- (Fig. 17).

Titration experiments showed that bam[6] binds halide anions in organic solvent mixtures (MeOD/ CDCl_3 , 2:1) and in aqueous media ($\text{D}_2\text{O}/\text{CD}_3\text{CN}$, 1:1), with the preference $\text{I}^- > \text{Br}^- > \text{Cl}^- > \text{F}^-$.^{4,29}

In 2011, the family of bambus[*n*]uril was extended for three analogs, of which two methyl groups of bam[6] were changed to benzyl or propyl groups, and for the third analog the macrocyclic ring only consisted of four glycouril monomers, the octabenzyl-bambus[4]uril (Fig. 18).³⁰

The propyl-bambus[6]uril (pro-bam[6]) showed similar binding affinities toward anions as the bam[6], whereas ben-bam[6] showed stronger binding for the halide anions than bam[6] together with better solubility in organic solvents. The ben-bam[4] did not show any binding to anions probably due the smaller cavity of the macrocycle. The ben-bam[6] crystallize with benzoates

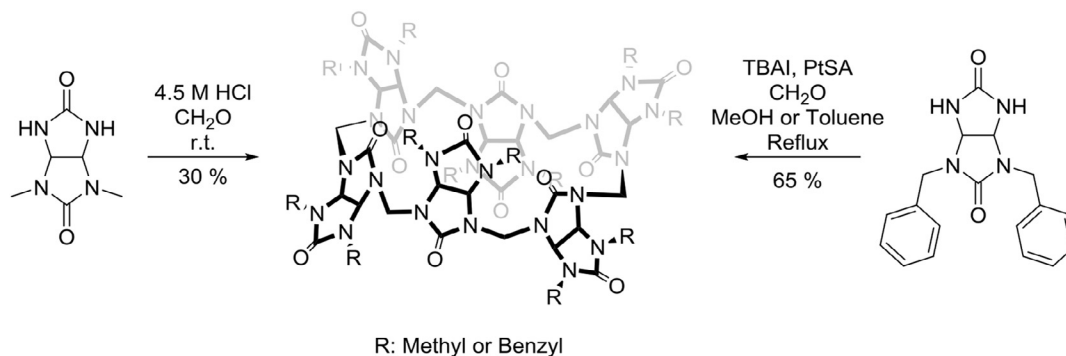


Figure 16 General bambus[6]uril synthesis.

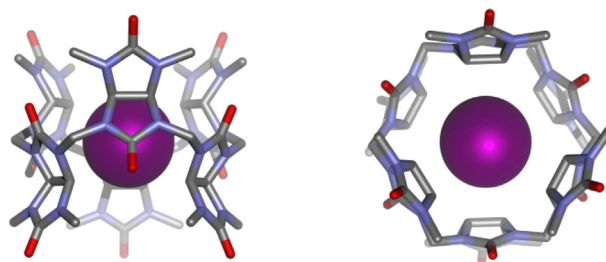


Figure 17 Single crystal X-ray structure of bambus[6]uril containing iodide (*left*: side view, *right*: top view).²⁹ Hydrogens and solvent molecules have been omitted for clarity.

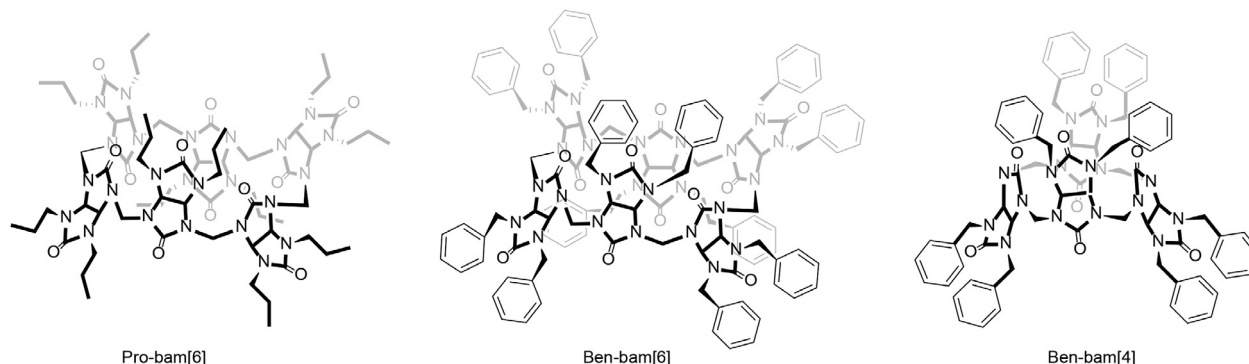


Figure 18 Structures of (*left to right*) propyl-bambus[6]uril, benzyl-bambus[6]uril, and benzyl-bambus[4]uril.

(or tosylates) in a 1:2 fashion, whereas in chloroform solution both 1:1 and 1:2 complexes were detected (**Fig. 19**).³¹ The distribution between the 1:1 and 1:2 complexes in chloroform solution was affected by the amount of water. Increasing the amount of water shifted the complex distribution toward the 1:2 complex (**Fig. 19**).

This observation fitted well with the single crystal X-ray structures as the two tosylates or benzoates are seen binding with a hydrogen of one water molecule which is situated in the center of the cavity of bambus[6]uril.

In 2012, Heck and coworkers produced five new members of the bambus[*n*]uril family, the octa-allyl-bambus[4]uril, dodeca-allyl-bambus[6]uril, octa-propen-bambus[4]uril, octa-propyl-bambus[4]uril, and a hepta-allyl-heptene-bambus[4]uril (selected macrocycles are shown in **Fig. 20**).³²

Heck used Grubbs II catalyst on the octa-allyl-bambus[4]uril and 1-heptene to synthesize the hepta-allyl-heptene-bambus[4]uril in 20% yield by metathesis (**Fig. 21**). Surprisingly, this reaction resulted in reaction of only one of the allyl groups to the heptene-yl group, and in this way the first unsymmetrical dialkyl-*N,N'*-ethyleneurea uril macrocycle was produced.

Heck also tried a ring closing metathesis of the octa-allyl-bambus[4]uril, using Hoveyda–Grubbs catalysts, but instead of the desired ring closed product, they obtained the isomeric product the octa-propenyl-bambus[4]uril in quantitative yields. Further, Heck and coworkers showed that the original bambus[6]uril synthesis by Sindelar could be improved from 65% to 90% yield by employing microwave conditions instead of conventional heating.

Until 2015, no thio analogs of bam[*n*], hmCB[*n*], cyhmCB[*n*], or even CB[*n*] had been prepared, even though calculations proposed that thio-CB[6] should be a stable molecule.³³ This was due to the fact that the thio-glycouril decomposes in acidic media, which so far has been the reaction medium of choice to produce these hexameric structures.³⁴ By methylation, and thereby protection of the nitrogens in the thio-urea part of the monothioglycouril yielded a mono-thio-glycouril analog, which has an increased

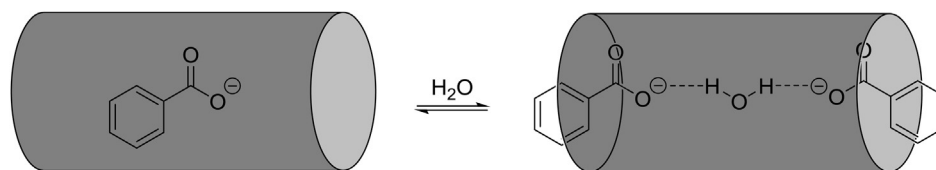


Figure 19 The distribution of 1:1 and 1:2 complexes between benzoate and dodecabenzyl-bambus[6]uril (*gray cylinder*) which is shifted by addition or removal of water.

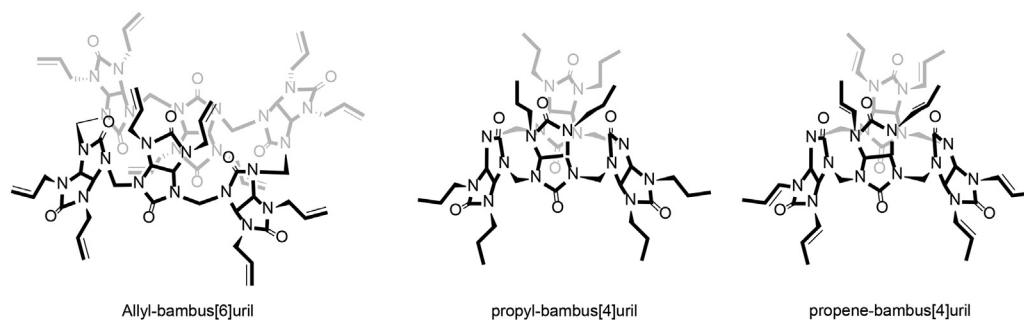


Figure 20 Schematic representation of selected bambus[6]uril analogs by Heck and coworkers (*left to right*) of the allyl-bambus[6]uril, propyl-bambus[4]uril, and propen-bambus[6]uril.

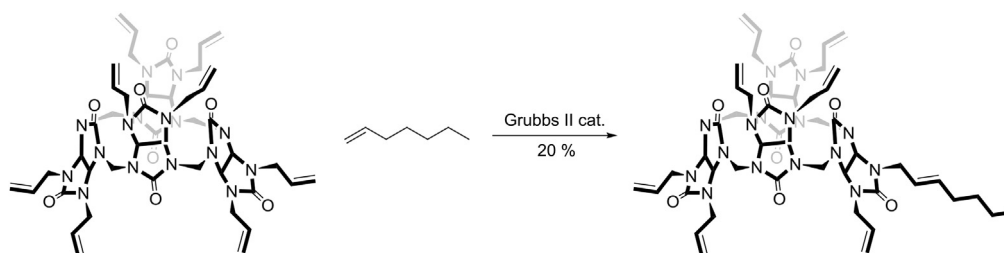


Figure 21 Heck's synthesis of a unsymmetric hepta-allyl-heptene-bambus[4]uril.

stability in acidic media. Using this protected mono-thio-glycouril, Reany and coworkers were able to produce the first thio-analog of bambus[4, 6]uril called semithiobambusurils (thio-bam[4, 6]), by employing Heck reaction conditions (Fig. 22).³⁵

The thio-bam[6] was also rather insoluble in organic solvents but addition of suitable anions increased the solubility in DMSO. The thio-bam[6] binds anions like the halides in the order $\text{Br}^- > \text{I}^- > \text{Cl}^-$ in DMSO, which is a bit different from bam[6]. The thio-bam[4] is able to bind soft thiophilic cations such as Hg^{2+} and Pd^{2+} as shown by ^1H -NMR spectroscopy and by single crystal X-ray structures (Fig. 23). Like for allyl-bambus[4]uril the cavity is too small to include anions (Fig. 24). The HgCl_2 is bound by the thio-bam[4] in linear chains of coordination polymers, where the sulfur is coordinating to the thiophilic Hg^{2+} cation.

By comparing the structures in Figs. 23 and 24, it is observed that the cavity size and shape of the thio-bam[4] does not change significantly, and that the cavity size prevents incorporations of even small anions such as Cl^- . The difference in the two crystal structures is that the HgCl_2 produces polymers with semithiobambus[4]uril, whereas no coordination polymers were seen when HgCl_2 is not present.

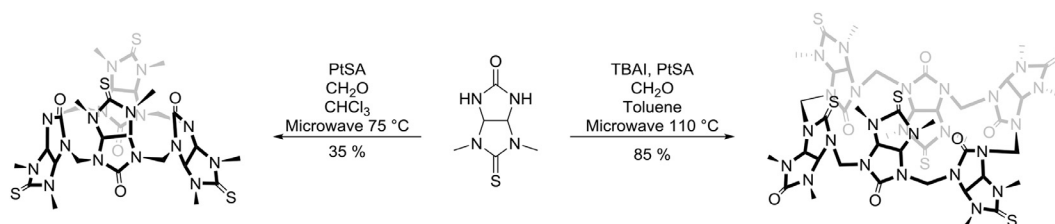


Figure 22 Synthetic pathway of the semithiobambus[4, 6]urils.

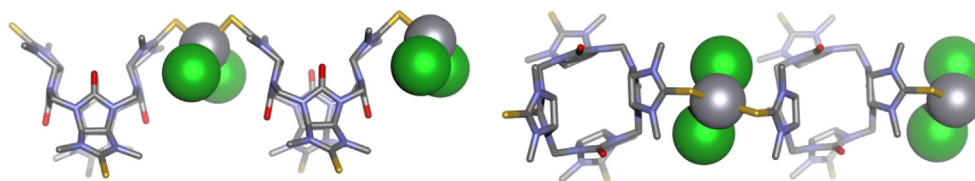


Figure 23 Part of the single crystal X-ray structure of the semithiobambus[4]uril HgCl_2 complex (left: side view, right: top view).³⁵ Hydrogens and solvent molecules have been removed for clarity.

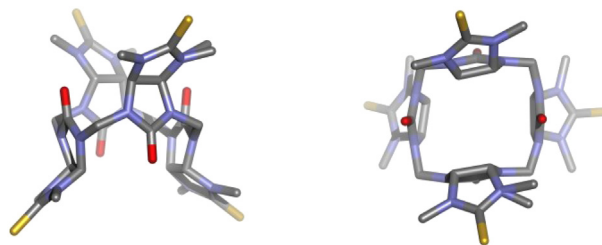


Figure 24 Single crystal X-ray structure of the semithiobambus[4]uril (*left*: side view, *right*: top view).³⁵ Hydrogens and solvent molecules have been removed for clarity.

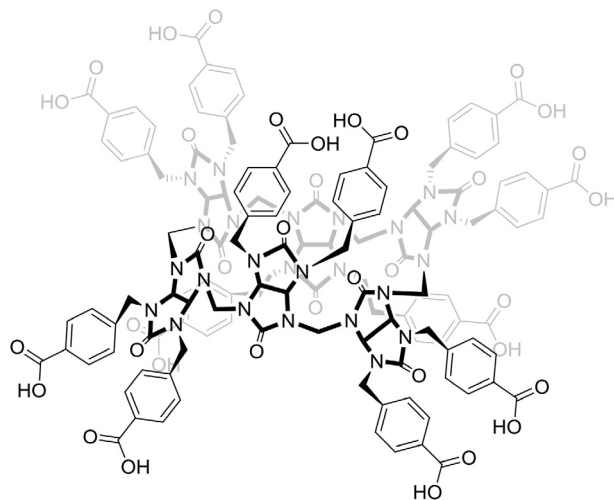


Figure 25 Water soluble bambus[6]uril.

In 2014, Sindelar and coworkers expanded the bambus[*n*]uril family with the first water soluble analog.¹² The benzyl groups on bambus[6]uril were changed to 4-carboxybenzyl to enable solubility in water (**Fig. 25**).

The binding interactions of the macrocycle spanned from $1.1 \times 10^2 \text{ M}^{-1}$ for F^- to impressive $1.0 \times 10^7 \text{ M}^{-1}$ for I^- in water at pH 7.1. These high binding affinities were obtained solely through C–H \cdots anion interactions. Again the preference for anion binding was $\text{I}^- > \text{Br}^- > \text{Cl}^- > \text{F}^-$, and as for the other bam[6]'s no cation binding was detected, and a change in pH did not change the binding interaction noticeably. The water soluble bambus[6]uril was later, in 2015, used to differentiate anions in water, by exploiting that the water soluble bambus[6]uril makes 1:1 complexes with slow exchange on the NMR chemical shift time scale.³⁶ Different anions produce different bambus[6]uril \supset anion peaks in the ^1H -NMR spectrum, and using these features it was possible to identify nine different anions in the same sample of $\text{DMSO}-\text{D}_2\text{O}$. Further, they were able to measure the concentration of the five different anions simultaneously in the same NMR sample within a 5% error.

Later, in 2015, the ben-bam[6] was seen to bind anions in chloroform with K_a values of $2.8 \times 10^{10} \text{ M}^{-1}$ for iodide.³⁷ Sindelar and Havel further found that the binding was enthalpy driven and typically an unfavorable entropy was observed. Also they found that in chloroform the ben-bam[6] makes 1:1 complexes with slow exchange, which again was used to identify different anions and their concentration within a 10% margin of error.

3.09.6 Biotin[6]uril

In 2014, the first water soluble macrocycle of the *N,N'*-ethylene urea family of receptors was presented by our group.⁵ Starting from D-biotin, also known as vitamin B7, a natural compound from the natural chiral pool of vitamins, we were able to synthesize biotin[6]uril (bio[6]).

The bio[6] was synthesized from a mixture of D-biotin and paraformaldehyde in 3.5 M H_2SO_4 with NaBr as a template, and was isolated as a single isomer in 63% yield (**Fig. 26**). The bio[6] consists of six D-biotin monomers situated in an alternating orientation of the carbonyl groups, which are connected through methylene bridges at the urea nitrogens. The alternating orientation produces a hydrophobic cavity that has 12 C–H moieties pointing toward the cavity. The cavity of biotin[6]uril has been observed to include molecules such as ethanol, water, and anions like iodide in the single crystal X-ray structures (**Fig. 27**).^{5,13}

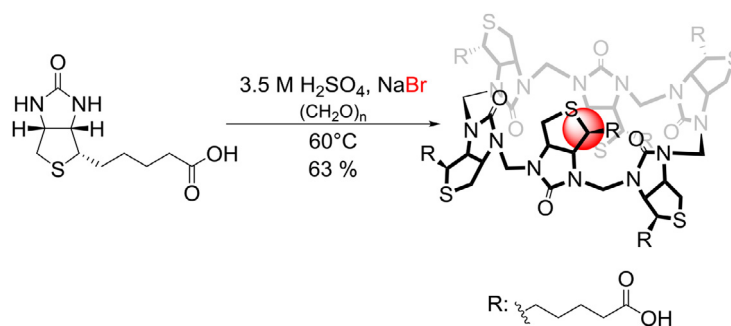


Figure 26 Synthetic pathway of the biotin[6]uril.

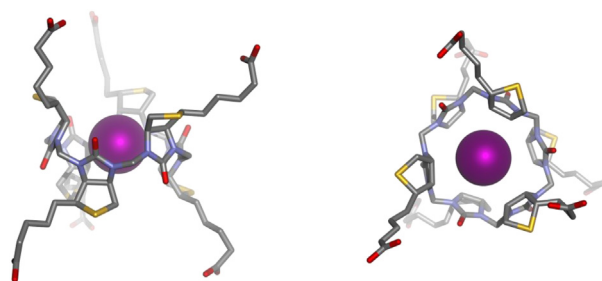


Figure 27 Single crystal X-ray structure of the biotin[6]uril binding iodide.⁵ Hydrogens, cation, and solvent molecules are omitted for clarity.

The 6+6 macrocycle has 18 chiral centers, 3 on each D-biotin monomer. Furthermore, the nonequivalence of the nitrogens in the D-biotin monomers gives the possibility of nine different regioisomers for the biotin[6]uril. Considering all the possible combinations of stereo- and regioisomers for the 6+6 macrocycle makes it very intriguing that only one isomer is isolated.

We found that the synthesis of bio[6] could be carried out in both 7 M HCl or 3.5 M H₂SO₄ and that it was templated by halide anions (Fig. 28). The isolated product contained the templated anion, for example, Cl[−] or Br[−], and the chloride could be removed

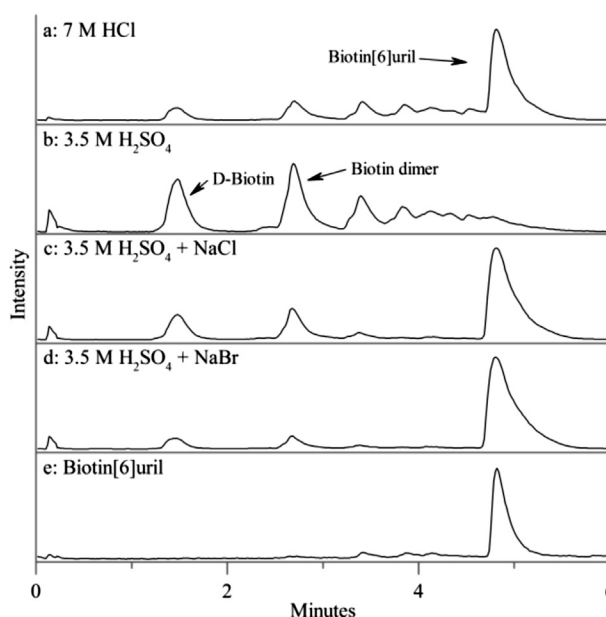


Figure 28 Extracted HPLC ion chromatograms of both cyclic and linear oligomers employing different reaction conditions. (A) 7 M HCl, (B) 3.5 M H₂SO₄, (C) 3.5 M H₂SO₄ + 7 M NaCl, (D) 3.5 M H₂SO₄ + 7 M NaBr, and (E) the isolated biotin[6]uril. All none marked peaks are smaller, linear, or cyclic products.

using TiNO_3 in alkaline solution followed by filtration and precipitation with acid. Later it was shown that the removal of Cl^- could be obtained through a simple acid–base recrystallization.¹⁴

Bio[6] binds monovalent anions in water (pH 7.5) with the preference for softer anions over harder, which can be seen from the preference $\text{SCN}^- > \text{I}^- > \text{Br}^- > \text{Cl}^-$.¹³ The stoichiometry of all the monovalent anions showed a 1:1 interaction as seen by studying the complexation using Job's method and by electrospray ionization mass spectrometry analysis. As many of the previously mentioned macrocycles, the bio[6] shows no interaction with cations such as Na^+ , K^+ , Cs^+ , and changing the pH, from pH = 7.5 to pH = 10.8 did not influence the binding isotherms. General for all the anion-binding interactions in water analyzed by isothermal calorimetry titration (ITC) is that the enthalpic contribution is favorable and large, whereas the entropic contribution is small and unfavorable.

Like the bambus[6]uril macrocycles, the biotin[6]uril binds anions through C–H \cdots anion interactions from the 12 hydrogens pointing toward the cavity. The crystal structure of bio[6] containing either EtOH, water, or iodide showed that the radius of the binding cavity is relatively constant as seen by solving the single crystal X-ray structure of a series of macrocycles-guest complexes (Fig. 29). The height of the cavity of the macrocycle can change by a small rotation the biotin monomers, which influences the total volume of the cavity. This small rotation will also change the orientation of the C–H interacting groups in the cavity, which thereby is able to change the binding site in order to get the optimal fit of a potential guest.

In order to rationalize the reaction pathway of the macrocyclization, we followed the reaction by the LC–MS analysis, and found that in the beginning of the reaction, mainly D-biotin and a linear dimer biotin[2]uril were observed (Fig. 30). After 2–4 h the biotin[6]uril started to appear, and after approximately 24 h became the major product, by a decrease in the amount of both the biotin monomer and the biotin[2]uril.

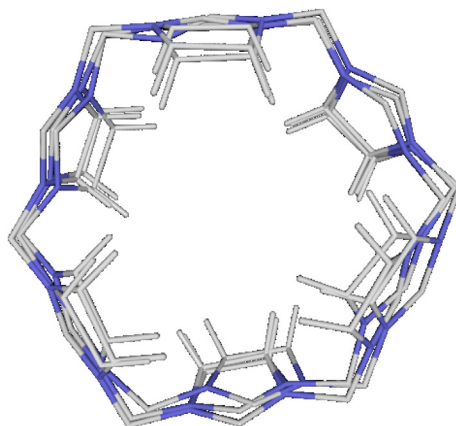


Figure 29 Overlay of the urea-part of the three crystal structures of biotin[6]uril showing that the diameter of the binding cavity only changes marginally with the three different guest molecules (iodide, EtOH, and water).^{5,13}

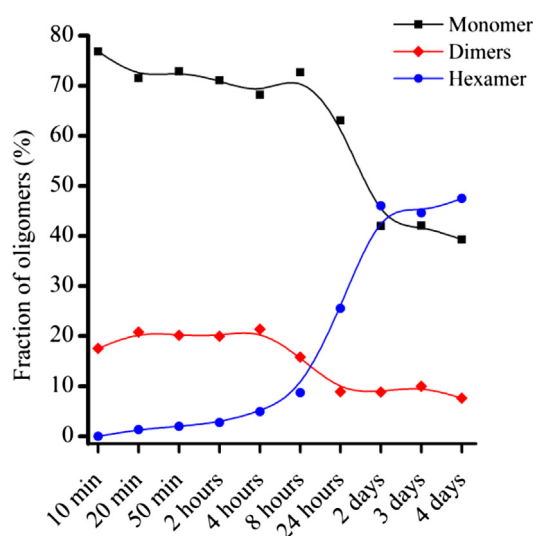


Figure 30 Evolution of the reaction between D-biotin and formaldehyde showing that biotin and the linear biotin[2]uril are consumed during the reaction. The reaction was followed by LC–MS at 209 nm.

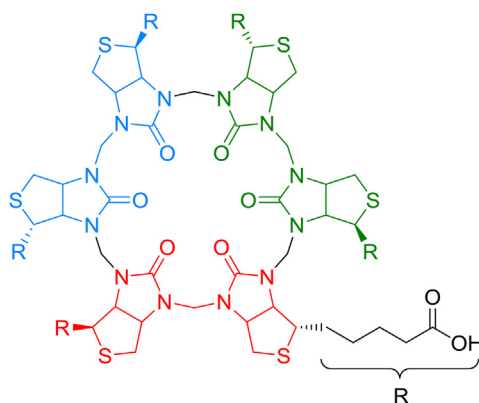


Figure 31 Schematic representation of biotin[6]uril showing three identical parts of the macrocycle which resembles the linear biotin[2]uril (*red*, *blue*, and *green*). The methylene bridges connecting the biotin[2]uril units are marked in *black*.

We were also able to isolate the linear biotin[2]uril from a mixture of D-biotin, a catalytic amount of H_2SO_4 , and paraformaldehyde (**Fig. 31**). The two biotin moieties in biotin[2]uril were connected at the two nitrogens furthest away from the alkyl chain of the D-biotin monomer. Due to the C_3 -symmetry of bio[6] it is possible to divide the macrocycle into three identical parts, where each contains exactly the linear biotin[2]uril connected by methylene bridges (**Fig. 32**).

These facts lead us to believe that the biotin[2]uril would be able to trimerize to the hexameric macrocycle biotin[6]uril, as this reaction pathway would also rationalize the high regioselectivity of the reaction. To test this hypothesis, the dimer was treated with 7 M HCl and paraformaldehyde. The result turned out to be the biotin[6]uril in similar yields as the synthesis starting from the biotin monomer. This indicates that the reaction is thermodynamically driven, and that the biotin[6]uril is the most stable product under the reaction conditions used.

In 2015, the bio[6] was made soluble in organic solvents by changing the carboxylic acids to the esters, methyl (bio[6]me), ethyl (bio[6]et), and butyl (bio[6]bu), respectively, by employing Fishers ester synthesis strategy directly on the biotin[6]uril (**Fig. 33**).¹⁴

By ^1H -NMR titrations and ITC experiments the binding interactions of the hexaesters to anions such as Cl^- , NO_3^- , HCO_3^- , and SO_4^{2-} were studied in acetonitrile. The biotin[6]uril hexaesters had comparable binding affinities whether the studies were done using bio[6]me, bio[6]et, or bio[6]bu for both chloride and nitrate. The binding interaction for chloride was also measured by ITC and it was found that both the enthalpy and entropy were favorable, which is different for bio[6] in water where the entropy was unfavorable.

Chloride was bound two orders of magnitude stronger than NO_3^- and HCO_3^- , whereas no binding was seen for the SO_4^{2-} anion. The selectivity for chloride over nitrate and bicarbonate is probably a consequence of hydrophilicity of the anions, as chloride is more hydrophilic than nitrate and bicarbonate.³⁸ Both nitrate and bicarbonate have almost the same K_a , and this peaked our

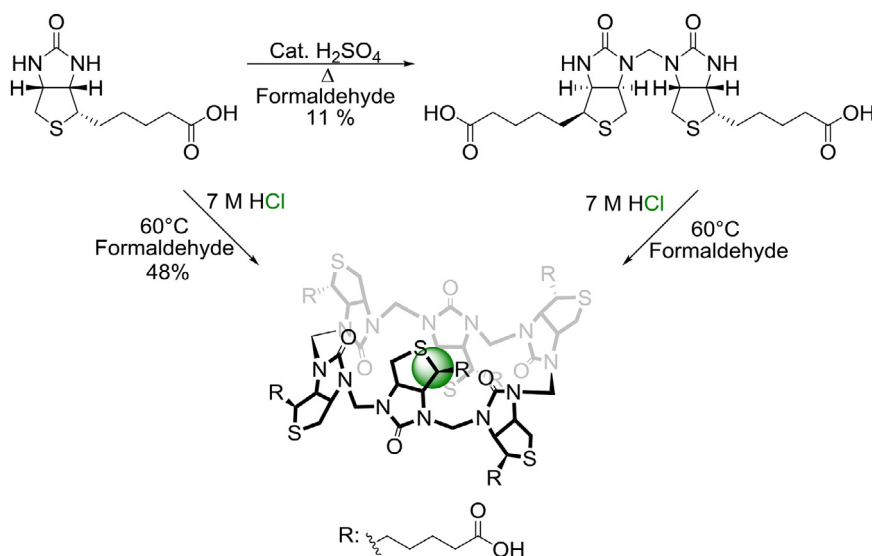


Figure 32 Synthetic pathway of the biotin[6]uril, starting from either D-biotin or biotin[2]uril.

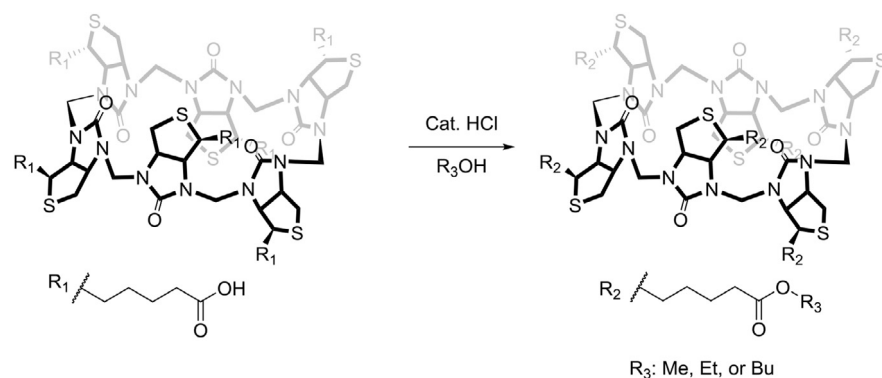


Figure 33 Synthetic strategy for the biotin[6]uril hexaesters.

hopes that the low affinities in none competitive medium would diminish the chances of extracting hydrophilic HCO_3^- from the water phase. HCO_3^- is far more basic, and therefore the better acceptor for conventional hydrogen bonds (HNO_3 $\text{p}K_a = -1.3$; H_2CO_3 $\text{p}K_a = 3.6$ and 10.3), so that NO_3^- and HCO_3^- having similar K_a values shows the difference between standard hydrogen bonding and $\text{C-H}\cdots\text{anion}$ interactions.³⁹

The anion transport capabilities of the biotin[6]uril hexaesters were tested using unilamellar vesicles consisting of POPC, cholesterol (70/30), and bio[6] hexaester employing the “Lucigenin assay,” where the chloride influx and nitrate efflux are monitored by a decrease in the emission from lucigenin due to the quenching by the increasing concentration of chloride within the vesicle cavity (Fig. 34).⁴⁰

When adding an external pulse of chloride, a decay in the emission at 535 nm was observed showing that the bio[6]esters were indeed transporting chloride into the vesicles employing $\text{C-H}\cdots\text{anion}$ interactions. All three esters (bio[6]me, bio[6]et, and bio[6]bu) showed transport, and increasing the lipophilicity by increasing the ester chain length showed enhanced transport rates with the butyl ester being the fastest (Fig. 35). Leaching experiments showed that the transporters were solely located in the vesicle membrane, and therefore the increased transport rate cannot be caused by a different distribution between the membrane and the aqueous phases. The transport rate of the bio[6]esters is of modest rates, but compares well with other conventional systems which employs $\text{N-H}\cdots\text{X}^-$ or $\text{O-H}\cdots\text{X}^-$ interactions for transport.^{41,42}

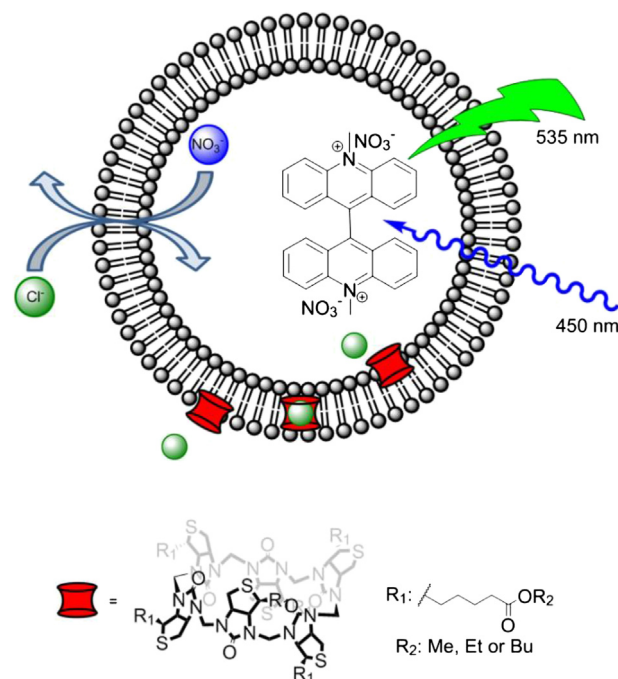


Figure 34 Schematic representation of the Lucigenin assay employed in the study of anion transport by biotin[6]uril hexaesters. Transport of Cl^- into the vesicles and NO_3^- out of the vesicles is monitored by the quenching of the lucigenin fluorescence caused by chloride inside the vesicle. In the lower part of the vesicle membrane is illustrating the carrier mechanism employed by the biotin[6]uril hexaesters.

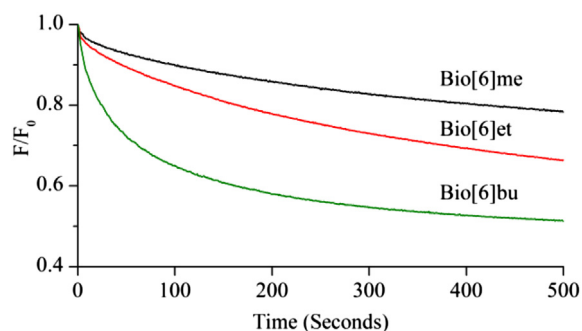


Figure 35 Chloride/nitrate exchange by biotin[6]uril hexaesters (methyl, ethyl, and butyl) at a transporter-to-lipid ratio of 1:1000.

Changing from NO_3^- to SO_4^{2-} in the lucigenin assay caused the transport to halt, which indicates that the biotin[6]uril hexaesters cannot transport intervesicular SO_4^{2-} out of the vesicles when Cl^- is transported in, whereas NO_3^- is able to be transported out of the vesicles in order to maintain electroneutrality. The change from nitrate to sulfate also shows that the biotin[6]uril hexaesters cannot transport Na^+ . Changing the counter anion transported in the lucigenin assay to HCO_3^- resulted in an almost identical transport rate as seen in the sulfate experiment. Thus, the experiment shows high selectivity for chloride transport over bicarbonate and sulfate transport.

The transport of anions using biotin[6]uril hexaesters was shown to occur via a carrier mechanism, by studying the system employing the lucigenin assay with different amounts of cholesterol in the vesicle membrane. By changing the amount of cholesterol the fluidity of the membrane should be changed, which in turn should affect carriers, whereas channels should be unaffected.⁴³ As expected for carriers, the transport rate was hampered when the cholesterol levels were increased. The transport mechanism was further tested, still using the lucigenin assay, but by employing vesicles composed of DPPC which is a gel phase at room temperature and a liquid crystalline phase above 41°C .⁴⁴ A carrier would be expected to not show any transport at room temperature but show transport at temperatures above 41°C , whereas channels should be unaffected by the temperature change. Again the carrier mechanism of transport for the biotin[6]uril hexaesters was confirmed as transport was observed at 45°C and not at 25°C .

The selectivity of biotin[6]uril hexaesters in both anion transport and anion binding could be a result of the “soft” nature of the C–H hydrogen bond relative to other hydrogen bond donors, which favors softer anions over hard anions (Cl^- over, eg, HCO_3^-). Even though anion transporters have employed C–H \cdots anion interactions in combination with N–H hydrogen bonding before,^{45,46} the biotin[6]uril hexaesters are the first anion transporters that solely rely on C–H \cdots anion interactions that enable selectivity. Furthermore, the C–H groups are not hydrophilic and therefore less prone to promote aggregation.

3.09.7 Outlook

The intriguing world of macrocycles is growing at a rapid pace, and the hexameric macrocycles that bind anions have been growing since the hemicucurbit[*n*]urils were first synthesized in 2004. Many of the macrocycles have the alternating orientation of the monomers that enable them to bind anions instead of cations like the cucurbit[*n*]uril. The anions are bound by C–H \cdots anion interactions, which have been shown to be effective in binding anions in both organic and aqueous solutions. A factor that might influence the strong binding affinities observed for the biotin[6]urils to the anions has recently been speculated to be the chaotropic and the nonclassical hydrophobic effect.^{13,15,47} All the members in the hemicucurbit[6]uril feature neutral hydrophobic binding pockets, and some members of the family have solubility in both water and organic solvents, which increase their applicability in bioorganic applications. Furthermore, all of the hemicucurbit[6]uril family members are synthesized by templated reactions typically with a halide as the template. The fact that the (*all-R*)-cychmCB[8] becomes the major product over the (*all-R*)-cychmCB[6] by changing the template suggests that many new macrocycles of different sizes can be produced in the future by changing the template, and thereby employing a dynamic combinatorial chemistry approach.^{48,49} A drawback of the hemicucurbit[6]uril family of macrocycles is the limit of direct functionalization; one exception is the transformation of biotin[6]uril to the corresponding esters. In particular, for the biotin[6]uril systems the possibilities for direct functionalization appear very attractive.

The possibility of chiral selectivity in molecular recognition could also be feasible, and initial efforts in this direction has been made by the synthesis of the chiral cyclohexylhemicucurbit[*n*]urils and biotin[6]urils.

The hemicucurbit[6]uril family will probably grow both in numbers and in ring sizes in the future due to their interesting anion-binding motifs. We predict that the use of these macrocyclic hosts will find applications in new areas such as biology, biochemistry, and other areas of science.

References

- Miyahara, Y.; Goto, K.; Oka, M.; Inazu, T. *Angew. Chem. Int. Ed.* **2004**, *43*, 5019–5022.
- Behrend, R.; Meyer, E.; Rusche, F. *Justus Liebigs Ann. Chem.* **1905**, 339, 1–37.
- Freeman, W. A.; Mock, W. L.; Shih, N. Y. *J. Am. Chem. Soc.* **1981**, *103*, 7367–7368.
- Svec, J.; Necas, M.; Sindelar, V. *Angew. Chem. Int. Ed.* **2010**, *49*, 2378–2381.
- Lisbjerg, M.; Jessen, B. M.; Rasmussen, B.; Nielsen, B. E.; Madsen, A.Ø.; Pittelkow, M. *Chem. Sci.* **2014**, *5*, 2647–2650.
- Aav, R.; Shmatova, E.; Reile, I.; Borissova, M.; Topić, F.; Rissanen, K. *Org. Lett.* **2013**, *15*, 3786–3789.
- Lagona, J.; Mukhopadhyay, P.; Chakrabarti, S.; Isaacs, L. *Angew. Chem. Int. Ed.* **2005**, *44*, 4844–4870.
- Kim, J.; Jung, I.-S.; Kim, S.-Y.; Lee, E.; Kang, J.-K.; Sakamoto, S.; Yamaguchi, K.; Kim, K. *J. Am. Chem. Soc.* **2000**, *122*, 540–541.
- Cao, L.; Šekutor, M.; Zavalij, P. Y.; Mlinarić-Majerski, K.; Glaser, R.; Isaacs, L. *Angew. Chem. Int. Ed.* **2014**, *53*, 988–993.
- Buschmann, H. J.; Cleve, E.; Schollmeyer, E. *Inorg. Chem. Commun.* **2005**, *8*, 125–127.
- Buschmann, H. J.; Zielesny, A.; Schollmeyer, E. *J. Incl. Phenom. Macrocycl. Chem.* **2006**, *54*, 181–185.
- Yawer, M. A.; Havel, V.; Sindelar, V. *Angew. Chem.* **2015**, *54*, 276–279.
- Lisbjerg, M.; Nielsen, B. E.; Milhoj, B. O.; Sauer, S. P. A.; Pittelkow, M. *Org. Biomol. Chem.* **2015**, *13*, 369–373.
- Lisbjerg, M.; Valkenier, H.; Jessen, B. M.; Al-Kerdi, H.; Davis, A. P.; Pittelkow, M. *J. Am. Chem. Soc.* **2015**, *137*, 4948–4951.
- Assaf, K. I.; Ural, M. S.; Pan, F.; Georgiev, T.; Simova, S.; Rissanen, K.; Gabel, D.; Nau, W. M. *Angew. Chem. Int. Ed.* **2015**, *54*, 6852–6856.
- Cong, H.; Yamato, T.; Feng, X.; Tao, Z. *J. Mol. Catal. A Chem.* **2012**, *365*, 181–185.
- Cong, H.; Yamato, T.; Tao, Z. *J. Mol. Catal. A Chem.* **2013**, *379*, 287–293.
- Cong, H.; Yamato, T.; Tao, Z. *New J. Chem.* **2013**, *37*, 3778–3783.
- Rowan, A. E.; Elemans, J. A. A. W.; Nolte, R. J. M. *Acc. Chem. Res.* **1999**, *32*, 995–1006.
- Volz, N.; Clayden, J. *Angew. Chem. Int. Ed.* **2011**, *50*, 12148–12155.
- Lee, J. W.; Kim, K.; Choi, S.; Ko, Y. H.; Sakamoto, S.; Yamaguchi, K.; Kim, K. *Chem. Commun.* **2002**, 2692–2693.
- Jeon, Y. J.; Bharadwaj, P. K.; Choi, S.; Lee, J. W.; Kim, K. *Angew. Chem. Int. Ed. Engl.* **2002**, *41*, 4474–4476.
- Xiang, D.-D.; Geng, Q.-X.; Cong, H.; Tao, Z.; Yamato, T. *Supramol. Chem.* **2014**, *27*, 37–43.
- Li, Y.; Li, L.; Zhu, Y.; Meng, X.; Wu, A. *Cryst. Growth Des.* **2009**, *9*, 4255–4257.
- Ören, M.; Shmatova, E.; Tamm, T.; Aav, R. *Phys. Chem. Chem. Phys.* **2014**, *16*, 19198–19205.
- Fomitsenko, M.; Shmatova, E.; Ören, M.; Järving, I.; Aav, R. *Supramol. Chem.* **2014**, *26*, 698–703.
- Prigorchenko, E.; Ören, M.; Kaabel, S.; Fomitsenko, M.; Reile, I.; Järving, I.; Tamm, T.; Topić, F.; Rissanen, K.; Aav, R. *Chem. Commun.* **2015**, *51*, 10921–10924.
- Fiala, T.; Sindelar, V. *Synlett* **2013**, *24*, 2443–2445.
- Svec, J.; Dusek, M.; Fejfarova, K.; Stacko, P.; Klán, P.; Kaifer, A. E.; Li, W.; Hudeckova, E.; Sindelar, V. *Chem. Eur. J.* **2011**, *17*, 5605–5612.
- Havel, V.; Svec, J.; Wimmerova, M.; Dusek, M.; Pojarova, M.; Sindelar, V. *Org. Lett.* **2011**, *13*, 4000–4003.
- Havel, V.; Sindelar, V.; Necas, M.; Kaifer, A. E. *Chem. Commun.* **2014**, *50*, 1372–1374.
- Rivollier, J.; Thuéry, P.; Heck, M.-P. *Org. Lett.* **2013**, *15*, 480–483.
- Pichierri, F. *Chem. Phys. Lett.* **2004**, *390*, 214–219.
- Singh, M.; Parvari, G.; Botoshansky, M.; Keinan, E.; Reany, O. *Eur. J. Org. Chem.* **2014**, *2014*, 933–940.
- Singh, M.; Solel, E.; Keinan, E.; Reany, O. *Chem. Eur. J.* **2015**, *21*, 536–540.
- Havel, V.; Yawer, M. A.; Sindelar, V. *Chem. Commun.* **2015**, *51*, 4666–4669.
- Havel, V.; Sindelar, V. *ChemPlusChem* **2015**, *80* (11), 1601–1606. <http://dx.doi.org/10.1002/cplu.201500345>.
- Sisson, A. L.; Clare, J. P.; Taylor, L. H.; Charmant, J. P. H.; Davis, A. P. *Chem. Commun.* **2003**, *17*, 2246–2247.
- Desiraju, G.; Steiner, T. *The Weak Hydrogen Bond: In Structural Chemistry and Biology T2*—International Union of Crystallography Monographs on Crystallography, Oxford University Press, 2001.
- McNally, B. A.; Koulov, A. V.; Smith, B. D.; Joos, J.-B.; Davis, A. P. *Chem. Commun.* **2005**, 1087–1089.
- Davis, J. T.; Okunola, O.; Quesada, R. *Chem. Soc. Rev.* **2010**, *39*, 3843–3862.
- Davis, A. P.; Sheppard, D. N.; Smith, B. D. *Chem. Soc. Rev.* **2007**, *36*, 348–357.
- Moore, S. J.; Haynes, C. J. E.; González, J.; Sutton, J. L.; Brooks, S. J.; Light, M. E.; Herniman, J.; Langley, G. J.; Soto-Cerrato, V.; Pérez-Tomás, R.; Marques, I.; Costa, P. J.; Félix, V.; Gale, P. A. *Chem. Sci.* **2013**, *4*, 103–117.
- Deng, G.; Dewa, T.; Regen, S. L. *J. Am. Chem. Soc.* **1996**, *118*, 8975–8976.
- Fisher, M. G.; Gale, P. A.; Hiscock, J. R.; Hursthouse, M. B.; Light, M. E.; Schmidtchen, F. P.; Tong, C. C. *Chem. Commun.* **2009**, 3017–3019.
- Yano, M.; Tong, C. C.; Light, M. E.; Schmidtchen, F. P.; Gale, P. A. *Org. Biomol. Chem.* **2010**, *8*, 4356–4363.
- Biedermann, F.; Nau, W. M.; Schneider, H.-J. *Angew. Chem. Int. Ed.* **2014**, *53*, 11158–11171.
- Rasmussen, B.; Sørensen, A.; Beeren, S. R.; Pittelkow, M. In *Organic Synthesis and Molecular Engineering*; John Wiley & Sons, 2013; pp 393–436.
- Corbett, P. T.; Leclair, J.; Vial, L.; West, K. R.; Wietor, J.-L.; Sanders, J. K. M.; Otto, S. *Chem. Rev.* **2006**, *106*, 3652–3711.